Kinematics and Statics Analysis of a Novel Cable-Driven Snake Arm Robot

Dawei Xu, En li, Zize Liang
State Key Laboratory of Management and Control for Complex Systems
Institute of Automation, Chinese Academy of Sciences, Beijing, 100190, China
University of Chinese Academy of Sciences, Beijing, 10090, China
Email: xudawei2015@ia.ac.cn, en.li@ia.ac.cn, zize.liang@ia.ac.cn

***Abstract*—Due to the great performance in complex and narrow spaces, snake-like robots, especially snake arm robots, have gained increasing attention in recent years. In this paper, a novel cable-driven snake arm robot is proposed. For greater flexibility, the snake arm not only has multiple two-degree-of-freedom joints, but also has telescopic modules that have one degree of freedom. The kinematics and statics analysis of n-module arm is performed. In kinematics analysis, the joint angles are used as an intermediate variables between the final pose and the cable lengths. And in order to get cable tension, the static equilibrium equations are used. At last, the simulation and results of a snake arm with two modules is given.**

***Index Terms*—Snake arm robot; Cable-driven; Telescopic module.**

I. Introduction

Recent years, there are numerous researches focus on the snake-like robots. One of the key advantages of snake-like robot is that it can be used in various complex spaces such as rescue, surgery, aircraft assembly, nuclear inspection, industrial exploration and so on [1],[2],[3].

According to the way of movement, snake like robots can be divided into bionic snake robots and snake arm robots. The bionic snake robots can move independently due to all the driving devices are placed inside the robot[4]. It is precisely because of this, these robots tend to use pneumatic or electric drivers[5]. Due to the lack of good end positioning ability and obstacle crossing ability, bionic snake robots can not be applied in complex tasks with obstacles and operation accuracy requirements. The snake arm robots usually fix their tails on feeding devices and remove their driving devices from of the arms, so they can use more complex driving devices and have high end positioning accuracy[6]. Most snake arm robots use cable-driven devices[2],[7],[8],[9], the significant advantage of this is that it can reduce the diameter and weight of the arm, so the robots can be more suitable for low access areas.

According to the way of structure, there are two kinds of snake arm robots: 1) continuous and 2) discrete. The arms of continuous robots are consisted of continuous structures[10],[11], so they can bend continuous and are usually considered as a whole in terms of analysis and control. In contrast, the arms of discrete robots are consisted of independent driving modules in series and each module can be considered as a rigid body[12], so the analysis and control methods are similar to super redundant manipulator and have higher end positioning accuracy relative to their continuous counterparts[13].

In this paper, the design and analysis of a discrete snake arm robot is presented, it has telescopic modules and compact layout of driving and feeding devices.

II. Mechanical Design

A. Design Principles

The proposed robot is used in industrial environment which is narrow and complex(Figure 1). These environments usually have irregular obstacles and gaps. In order to get to the expect position, the robot must have high flexibility to through these obstacles and gaps.

Fig. 1: Application environment

Further, because the forward or backward movement of the arm is driving by feeding device, so there must be enough space to accommodate the feeding device. The frequently used feeding device is a king of horizontal feeding device. Such devices tend to have a large volume due to the need to carry the driving device and arm. That means although the arm can extend into the narrow spaces, but the rest of the robot must be placed in an open space, this will cause the increasing of length of the arm. In order to get a higher availability under a certain length of arm, the space that feeding device needed should as smaller as possible.

Therefore, the proposed robot has a rotary feeding device to reduce the necessary space, and it also uses telescopic modules to cooperate with the rotary feeding device to rolling

978-1-5386-3524-7/17/$31.00 ©2017 IEEE

up the whole arm around the driving device and getting higher flexibility.

B. Mechanical Structure

The whole robot is shown in Figure 2. The feeding device has three parts: 1) the rotation motor is connected to the upper end of the support shaft, 2) the support shaft passes through the driving device, and the lower end of it is connected to 3) the chassis. The driving device is fixed on the support shaft, so that it can be rotated by the feeding device, therefore the arm which connected to the bottom edge of the driving device can be rolled up or unfold. The chassis of feeding device can protect the arm at downtime.

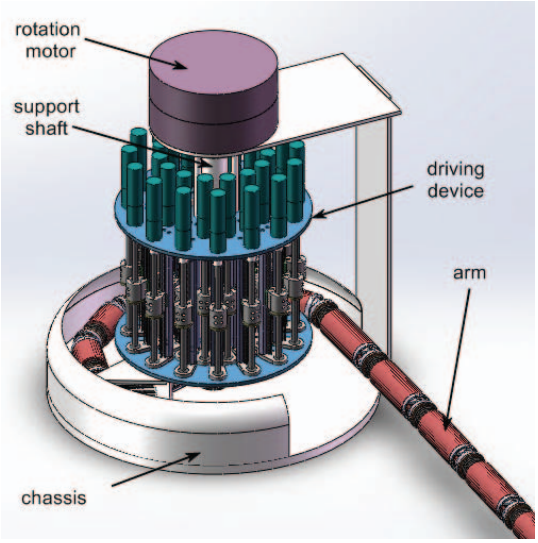

Fig. 2: The proposed robot

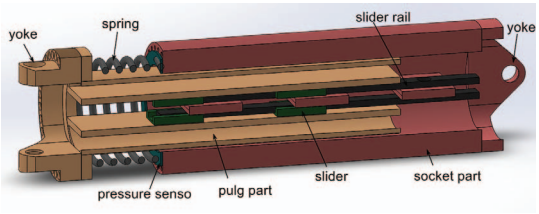

Fig. 3: The telescopic module

The telescopic module of the arm is shown in Figure 3, it is constructed of two part: 1) the plug part, which has two pair of sliders, inserts into the 2) socket part, which has a pair of slide rails at the corresponding location. Therefore, the plug part and the socket part can move in the axial direction. The spring between these two parts is used to work with the driving device to control the stretching and its pressure can be measured by the film pressure sensor.

In the opposite end of the two parts, each has a rigid plate on which is a yoke of the universal joint. The yoke can be combined with another yoke of other module to form a complete universal joint, which could be controlled by three cables that connected to the plate of the plug part, as shown in Figure 4.

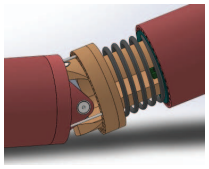

Fig. 4: The universal joint

III. Kinematics Formulations

As the robot is driven by cables, in addition to analyzing the relationship between joint angles and final pose, the cable lengths should given by the corresponding joint angles.

A. Single Module Analysis

1) Determination of kinematics transformation matrix: The final pose of module could be got by three coordinate transformation, as shown in Figure 5.

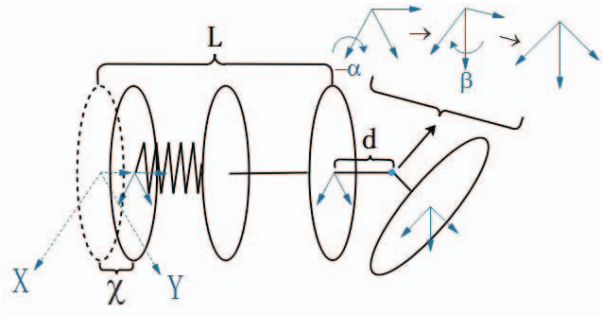

Fig. 5: Transformation of module

The first translation transformation is performed by spring:

$$T_{trans1} = Trans(0,0,L-\chi+d) = \begin{bmatrix} 1 & 0 & 0 & 0 \\ 0 & 1 & 0 & 0 \\ 0 & 0 & 1 & L-\chi+d \\ 0 & 0 & 0 & 1 \end{bmatrix} \quad (1)$$

here, L is the axial length between the yoke of plug part and the yoke of socket part at the initial position and χ is the compression length of the spring relative to the initial position.

The second rotation transformation is performed by universal joint:

$$T_{rotation} = Rot(X,\alpha)Rot(Y,\beta) = \begin{bmatrix} cos(\beta) & 0 & sin(\beta) & 0 \\ sin(\alpha)sin(\beta) & cos(\alpha) & -sin(\alpha)cos(\beta) & 0 \\ -cos(\alpha)sin(\beta) & sin(\alpha) & cos(\alpha)cos(\beta) & 0 \\ 0 & 0 & 0 & 1 \end{bmatrix} \quad (2)$$

here, α is the rotation angle of the universal joint around the X axis and β is the rotation angle around the Y axis.

The final translation transformation is a fixed one:

$$T_{trans2} = Trans(0,0,d) \quad (3)$$

here, d is the length of universal joint yoke.

Hence, the whole transform is :

$$T = T_{trans1} T_{rotation} T_{trans2} \tag{4}$$

2) Determination of cable lengths: A cable within a module is divided into two parts, shown in Figure 6.

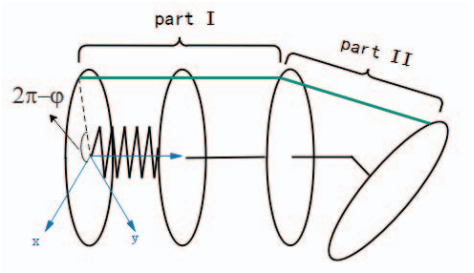

Fig. 6: Two part of a cable

The cable length of part I is:

$$l_I = L - \chi \tag{5}$$

The cable length of part II is determined by the rotation of universal joint, which shown in Figure 7.

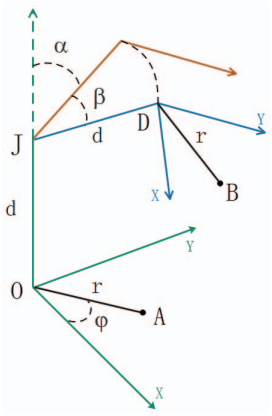

Fig. 7: The cable length of part II in universal joint

The length of $\overrightarrow{AB}$ represents the l_{II}. According to the Vector algebra, there is:

$$\overrightarrow{AB} = \overrightarrow{AO} + \overrightarrow{OJ} + \overrightarrow{JD} + \overrightarrow{DB} \tag{6}$$

where

$$\overrightarrow{OA} = r * R_z(\varphi) * [1,0,0]^T$$
$$\overrightarrow{OJ} = d * [0,0,1]^T$$
$$\overrightarrow{JD} = d * R_x(\alpha) * R_y(\beta) * [0,0,1]^T$$
$$\overrightarrow{DB} = r * R_x(\alpha) * R_y(\beta) * R_z(\varphi) * [1,0,0]^T$$

here, r is the radius of plate, A is the point of cable through-hole, B is the cable attachment point and φ is the right-handed angle from the X axis to A. For a certain module, d and r are constants and for a certain cable, φ is constant;

Therefore, the l_{II} is determined as follow:

$$l_{II} = f(\alpha, \beta, \varphi) = \|\overrightarrow{AB}\| \tag{7}$$

and the length of the i[th] cable of the module is:

$$l_i = f(\alpha, \beta, \varphi_i) + L - \chi \tag{8}$$

The attachment points of these driving cables are equally placed on the plate at 120° intervals, and so do the through-holes, therefore:

$$\varphi_i = \varphi_1 + i\frac{2}{3}\pi, (i = 2, 3) \tag{9}$$

B. Multiple Module Analysis

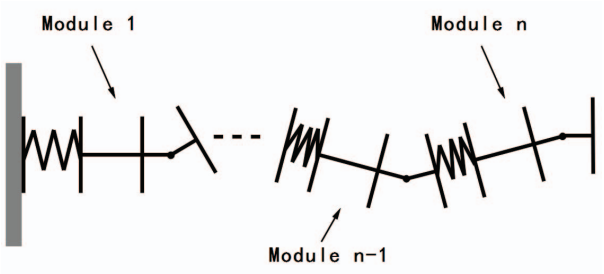

Fig. 8: Multiple modules

When there are n modules connected together in serially, as shown in Figure 8, the posture of pre-order modules should be considered to get the whole length of a module's driving cable. For a certain cable, the corresponding φ is a fixed value for every module it passed, so for the i[th] cable of the n[th] module, the length of it is :

$$l_{n,i} = \sum_{j=1}^{n} [f(\alpha_j, \beta_j, \varphi_{n,i}) + L - \chi_j] \tag{10}$$

The relationship of each module's coordinate system is conjoined coordinate system, so the final pose of n[th] module in the global coordinate system is determined by:

$$T(\theta) = T_1 T_2 T_3 \cdots T_n = \begin{bmatrix} n_x & o_x & q_x & p_x \\ n_y & o_y & q_y & p_y \\ n_z & o_z & q_z & p_z \\ 0 & 0 & 0 & 1 \end{bmatrix} \tag{11}$$

here, θ represent the joint angles of robot:

$$\theta = (\chi_1, \alpha_1, \beta_1, \cdots, \chi_n, \alpha_n, \beta_n)^T; \tag{12}$$

Due to the proposed robot is a super redundant robot, it is very difficult to get the closed-form solutions of inverse kinematics, but because the transform matrix of kinematics is known, the inverse kinematics could be solved by kinds of numerical solutions[14][15].

In order to find the values of joint angles for the target pose T_{target}, define:

$$S(\theta) = (p_x, p_y, p_z, n_x, n_y, n_z, o_x, o_y, o_z, q_x, q_y, q_z)^T \tag{13}$$

which represent the pose of robot and define:

$$E(\theta) = S_{target} - S(\theta) \tag{14}$$

then use the following equation to update the θ until (14) is within the allowable range of error, thus the θ for T_{target} is found.

$$\theta = \theta + \Delta\theta \tag{15}$$

$$\Delta\theta = J^{\dagger}E \tag{16}$$

here, $J^{\dagger}$ is the $pseudoinverse$ of the Jacobian matrix of robot:

$$J(\theta) = \left(\frac{\partial S_i}{\partial \theta_j}\right)_{i,j} \tag{17}$$

IV. Statics Analysis

It is worth noting that in the process of inverse kinematics solving, some joint angles that may break the static equilibrium or cause the cable tension over safe range should be avoided.

The static equilibrium has two conditions: 1) the external forces are balanced and 2) the torques are balanced.

A. Forces balance

To aid the force analysis, a simplified module is shown in Figure 9. It is important to note that the structure of the module in this section is different from the one in section III.

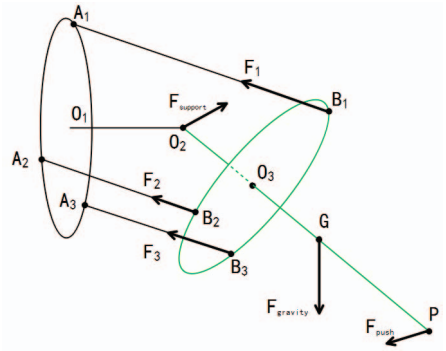

Fig. 9: Module force diagram

As a whole, the module (green) has 6 forces applied on it: 1) the support force from previous module, 2) the gravity of itself 3) the push force from next module and 4) the three pull forces from the driving cables. Due to the support force could change its direction and magnitude correspondingly, so the module can reach the force balance state, which means :

$$\overrightarrow{F_{support}} + \overrightarrow{F_{push}} + \overrightarrow{F_{gravity}} + \sum_{i=1}^{3} \overrightarrow{F_i} = 0 \tag{18}$$

the $\overrightarrow{F_{push}}$ of a module is the reaction force of the $\overrightarrow{F_{support}}$ of its next module and the $\overrightarrow{F_{push}}$ of n[th] module is zero.

And consider the spring push force, there is:

$$f_{support.O_2O_3} = f_{spring} = k\chi \tag{19}$$

here, k is the stiffness factor of spring, $f_{support.O_2O_3}$ is the magnitude of the $F_{support}$ in the direction O_2O_3.

B. Torques balance

The torques balance means that the sum of the torques about any axis of rotation is zero:

$$\sum \tau = 0 \tag{20}$$

here

$$\tau = \overrightarrow{Or} \times \overrightarrow{F} \tag{21}$$

and the $\overrightarrow{Or}$ is the vector from axis of rotation to the force applied point r.

For a certain point P, the $\overrightarrow{Or}$ can be written as:

$$\overrightarrow{Or} = \overrightarrow{OP} + \overrightarrow{Pr} \tag{22}$$

than, substituting (22) into (21)

$$\overrightarrow{\tau} = \overrightarrow{OP} \times \overrightarrow{F} + \overrightarrow{Pr} \times \overrightarrow{F} \tag{23}$$

let $\overrightarrow{\tau'} = \overrightarrow{Pr} \times \overrightarrow{F}$ and substituting it and (23) into (20)

$$\sum \tau = \overrightarrow{OP} \times \sum \overrightarrow{F} + \sum \tau' = 0 \tag{24}$$

As previously analyzed, the module can reach the force balance state, which means that $\sum \overrightarrow{F} = 0$, so the torque balance condition can be simplified as:

$$\sum \tau = \sum \tau' = 0 \tag{25}$$

which means that when the force is balanced, the torque balanced is independent of the position of rotation axis.

According to the mechanical structure, the module could only rotate around the rotation axis of universal joint (O_2), so the sum of torques about this point will be analyzed.

As shown in Figure 9, the applied point of support force is the rotation axis O_2, so its torque is :

$$\tau_{support} = 0 \tag{26}$$

And because of the applied point of push force P, the gravity point G, the center of plate O_3 and the rotation axis O_2 are collinear, there is :

$$\begin{aligned} \overrightarrow{O_2P} &= \varepsilon \overrightarrow{O_2O_3} \\ \overrightarrow{O_2G} &= \sigma \overrightarrow{O_2O_3} \end{aligned} \tag{27}$$

and then :

$$\begin{aligned} \tau_{push} + \tau_{gravity} &= \overrightarrow{O_2P} \times \overrightarrow{F_{push}} + \overrightarrow{O_2G} \times \overrightarrow{Gravity} \\ &= \overrightarrow{O_2O_3} \times \overrightarrow{F_{virtual}} \end{aligned} \tag{28}$$

$F_{virtual}$ is a imaginary force that used to replace the $\varepsilon * \overrightarrow{F_{push}} + \sigma * \overrightarrow{Gravity}$ and for certain mechanical structure, ε and σ are constants.

Therefore, for the module's torque analysis, the force diagram can be simplified as Figure 10.

The torque balance can be written as :

$$\begin{aligned} \tau_{sum} &= \sum_{i=1}^{3} \tau_i + \tau_{virtual} \\ &= \sum_{i=1}^{3} (\overrightarrow{O_2B_i} \times \overrightarrow{F_i}) + \overrightarrow{O_2O_3} \times \overrightarrow{F_{virtual}} = 0 \end{aligned} \tag{29}$$

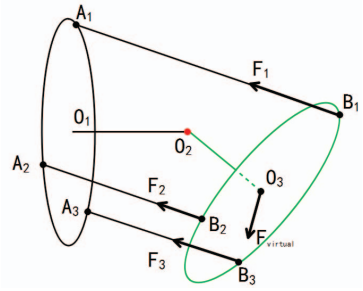

Fig. 10: Module torque diagram

Finally, combine (18), (19) and (29), the F_i and $F_{support}$ can be solved.

V. Simulation and Discussion

A. Simulation and results

According to the kinematics in section III, a arm consisting of two modules is built. The mechanical parameters of arm is:

TABLE I: The mechanical parameters of simulation

Parameters	r	d	L	φ_1	φ_2
Values	30 mm	10 mm	150 mm	0°	60°

The simulation task is to move the end of arm along a particular curve while the normal vector of end hold on $[0, 0, 1]^T$. The curve is:

$$\begin{cases} x = t^3/1500 \\ y = -t \qquad (-25 < t < 25) \\ z = 300 \end{cases}$$

The results of simulation is shown in Figure 11 $\sim$ Figure 15.

B. Discussion

Due to the normal vector of end remains to $[0, 0, 1]^T$, the rotation of module 2 always counteracts the rotation of module 1, as shown in Figure 12, the α_1, β_1 and α_2, β_2 are opposite to each other. For the same reason, the cable length differences caused by the module 1 are made up by module 2, so the cable lengths of module 2 in Figure 14b are almost always the same.

The curve on XY view in Figure 11 shows that the speed of end in X axis is faster than the speed in Y axis direction, this is caused the trajectory of β bend towards zero compare to α.

Because the end track in Z axis is always 300, each module shortens its length correspondingly when the end is near $[0, 0, 300]^T$, as shown in Figure 13.

The φ of the first cable of module 1 is 0, so its length is more affected by the α_1. Therefore, in Figure 14a, the trajectory of its length is almost a straight line. For the same reason, as shown in Figure 15a, it carries more gravity, and so do the first and third cable of module 2 in Figure 15b.

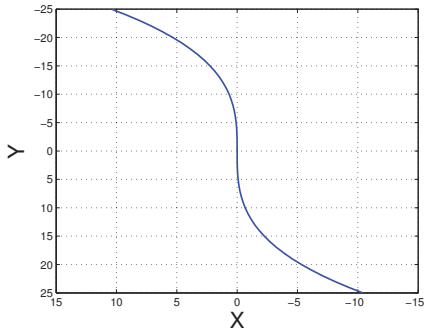

Fig. 11: The end track on XY view

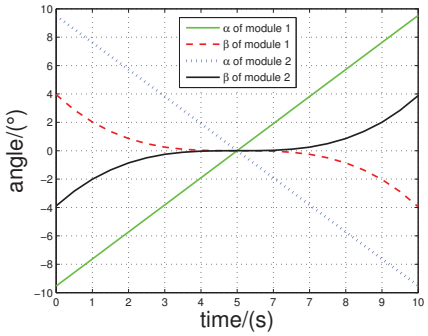

Fig. 12: α, β track

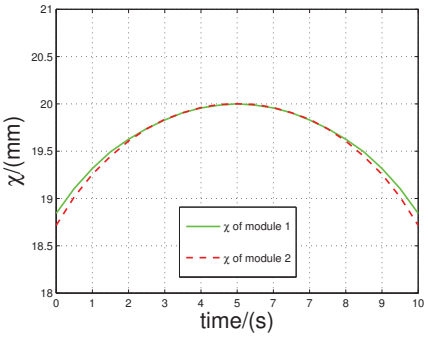

Fig. 13: χ track

VI. Future Prospects

In this paper, we propose a snake arm robot, which can rolled up itself to reduce the space requirement and get higher flexible via telescopic modules, and we also analyze the kinematics and statics of this robot. Comparing with the other cable driven modules, the proposed module increases a degree of freedom without increasing the number of cables. In theory, the robot will have more flexibility, but also it will be more difficult to control it. For future work, the control system and driving devices will be built to verify the flexibility of the arm, especially the stretch of modules. In addition, the influences caused by the forces, which cables applied on the modules them passed, are ignored in this paper, these deviations should be compensated in some way if higher position accuracy is desired.

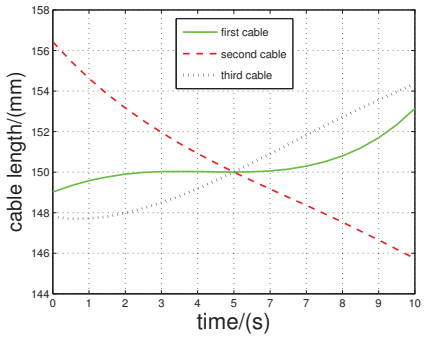

(a) Module 1

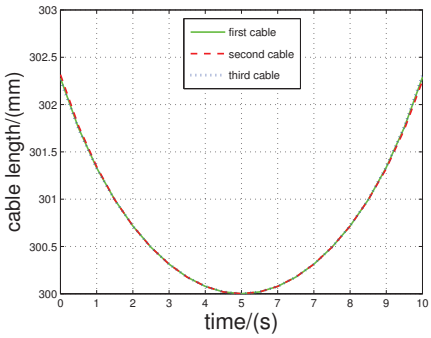

(b) Module 2

Fig. 14: Cable lengths

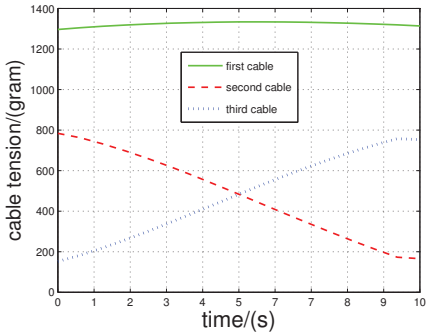

(a) Module 1

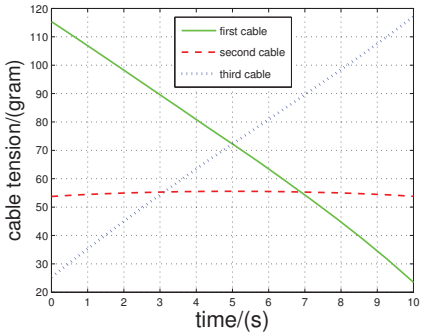

(b) Module 2

Fig. 15: Cable tension

ACKNOWLEDGMENT

This work is supported by National Natural Science Foundation of China under Grant 61403372,61403374, and by National Science and Technology Support Program of China under Grant 2015BAK06B01.

REFERENCES

[1] L. Chenguang, L. Jianyong, Z. Mingyuan, and W. Long, "Design of a portable snake-like search and rescue apparatus used in the gap," in *Mechatronic Science, Electric Engineering and Computer (MEC), 2011 International Conference on*. IEEE, 2011, pp. 676–679.

[2] H. Hu, P. Wang, B. Zhao, M. Li, and L. Sun, "Design of a novel snake-like robotic colonoscope," in *Robotics and Biomimetics (ROBIO), 2009 IEEE International Conference on*. IEEE, 2009, pp. 1957–1961.

[3] R. Buckingham, V. Chitrakaran, R. Conkie, G. Ferguson, A. Graham, A. Lazell, M. Lichon, N. Parry, F. Pollard, A. Kayani *et al.*, "Snake-arm robots: a new approach to aircraft assembly," SAE Technical Paper, Tech. Rep., 2007.

[4] D. Rollinson, Y. Bilgen, B. Brown, F. Enner, S. Ford, C. Layton, J. Rembisz, M. Schwerin, A. Willig, P. Velagapudi *et al.*, "Design and architecture of a series elastic snake robot," in *Intelligent Robots and Systems (IROS 2014), 2014 IEEE/RSJ International Conference on*. IEEE, 2014, pp. 4630–4636.

[5] C. Wright, A. Johnson, A. Peck, Z. McCord, A. Naaktgeboren, P. Gianfortoni, M. Gonzalez-Rivero, R. Hatton, and H. Choset, "Design of a modular snake robot," in *Intelligent Robots and Systems, 2007. IROS 2007. IEEE/RSJ International Conference on*. IEEE, 2007, pp. 2609–2614.

[6] R. Buckingham and A. Graham, "Dexterous manipulators for nuclear inspection and maintenancełcase study," in *Applied Robotics for the Power Industry (CARPI), 2010 1st International Conference on*. IEEE, 2010, pp. 1–6.

[7] Z. Zhang, G. Yang, S. H. Yeo, W. B. Lim, and S. K. Mustafa, "Design optimization of a cable-driven two-dof joint module with a flexible backbone," in *Advanced Intelligent Mechatronics (AIM), 2010 IEEE/ASME International Conference on*. IEEE, 2010, pp. 385–390.

[8] Y. Yao, Z. Du, and Z. Wei, "Research on snake-arm robot assmbly system," *Aviation Manufacturing Technology*, vol. 491, no. 21, pp. 26–30, 2015.

[9] I. P. Georgilas and V. D. Tourassis, "Ermis-a novel biologically inspired flexible robotic mechanism for industrial applications," in *Advanced Intelligent Mechatronics, 2009. AIM 2009. IEEE/ASME International Conference on*. IEEE, 2009, pp. 1504–1509.

[10] D. B. Roppenecker, L. Schuster, J. A. Coy, M. F. Traeger, K. Entsfellner, and T. C. Lueth, "Modular body of the multi arm snake-like robot," in *Robotics and Biomimetics (ROBIO), 2014 IEEE International Conference on*. IEEE, 2014, pp. 374–379.

[11] D. B. Roppenecker, A. Pfaff, J. A. Coy, and T. C. Lueth, "Multi arm snake-like robot kinematics," in *Intelligent Robots and Systems (IROS), 2013 IEEE/RSJ International Conference on*. IEEE, 2013, pp. 5040–5045.

[12] G. Lum, S. Mustafa, H. Lim, W. Lim, G. Yang, and S. Yeo, "Design and motion control of a cable-driven dexterous robotic arm," in *Sustainable Utilization and Development in Engineering and Technology (STUDENT), 2010 IEEE Conference on*. IEEE, 2010, pp. 106–111.

[13] L. Tran, Z. Zhang, S. Yeo, Y. Sun, and G. Yang, "Control of a cable-driven 2-dof joint module with a flexible backbone," in *Sustainable Utilization and Development in Engineering and Technology (STUDENT), 2011 IEEE Conference on*. IEEE, 2011, pp. 150–155.

[14] S. R. Buss, "Introduction to inverse kinematics with jacobian transpose, pseudoinverse and damped least squares methods," *IEEE Journal of Robotics and Automation*, vol. 17, no. 1-19, p. 16, 2004.

[15] N. N. Son, H. P. H. Anh, and T. D. Chau, "Inverse kinematics solution for robot manipulator based on adaptive mimo neural network model optimized by hybrid differential evolution algorithm," in *Robotics and Biomimetics (ROBIO), 2014 IEEE International Conference on*. IEEE, 2014, pp. 2019–2024.